

Experimental Shielding Effectiveness Analysis of Impact Hexagonal Air-vent Distances on a Metal Enclosure

Nataša Nešić¹, Nebojša Dončov², Slavko Rupčić³, Bratislav Milovanović⁴ and Vanja Mandrić Radivojević⁵

Abstract – In this paper the shielding effectiveness of metal enclosure with twelve hexagonal air-vents are experimentally studied. Therefore, two scenarios of hexagonal groups formed in 3x4 and 4x3 order are conducted. The experimental procedure is carried out in a semi-anechoic room. All measurement results are compared to the numerical ones obtained by TLM method with incorporated compact air-vent model and wire model.

Keywords – Shielding effectiveness, TLM hexagonal air-vent model, TLM wire model, Experimental analysis.

I. INTRODUCTION

To get protected from external influences, electronic equipment is usually placed inside some protective enclosures. The effect of these enclosures is two-fold. On the one hand, it is necessary to protect the electronic equipment inside enclosure from the outer radiation. On the other hand, the electromagnetic (EM) field which is generated from the electronic equipment inside enclosure should be reduced, as much as it is possible [1]. Commonly, shielding enclosures are made of a highly conductive material in order to reduce not only external EM fields impact on equipment inside the enclosure, but also a level of internal EM interferences emitted from equipment to outside space. Moreover, on the enclosures there usually exist the airflow aperture arrays of different shapes, so-called air-vents, as well as some other slots, which are intended for heating dissipation and airing [2].

To determine the shielding effectiveness (SE) characteristic of a metal enclosure over a frequency range, there exist several different methods, such as the analytical, the numerical and the experimental ones. There are many numerical methods that can be employed, e.g. Finite Difference Time Domain (FDTD) method in [3], Method of Moments (MoM) [4] and Transmission Line–Matrix (TLM) [5], etc. In the experimental methods, an antenna is set inside the enclosure in order to determine its SE. Usually, the monopole [6], and the dipole antenna [7] are used to

¹Nataša Nešić is with the College of Applied Technical Sciences Niš, Aleksandra Medvedeva 20, Niš 18000, Serbia, E-mail: natasa.bogdanovic@vtsnis.edu.rs

²Nebojša Dončov is with the Faculty of Electronic Engineering in Niš, University of Niš, Aleksandra Medvedeva 14, Niš 18000, Republic of Serbia, E-mail: nebojsa.doncov@elfak.ni.ac.rs

⁴Bratislav Milovanović is with the University of Singidunum, Danijelova 32, Belgrade 11000, Serbia, E-mail: bmilovanovic@singidunum.ac.rs

³Slavko Rupčić and ⁵Vanja Mandrić Radivojević and are with Department of Communications Faculty of Electrical Engineering Osijek 31000, Croatia, E-mails: rupcic@etfos.hr vanja.mandric@etfos.hr

determine the electric field level as opposite to the loop antenna which is appropriate to determine the magnetic field [6]. In [8] the impact of the physical dimensions of receiving antenna on the resonant frequency is also analyzed by using the TLM method.

The objective of this paper is to experimentally quantify the SE of a metallic enclosure with groups of 4x3 hexagonal air-vents on the removable front panel for one scenario and groups of 3x4 hexagonal air-vents for another scenario. Afterwards, these measurement results are compared to the numerical results obtained by the TLM method with incorporated compact wire model [8], [9] and hexagonal air-vent model [10], [11]. Namely, in the numerical simulations, the physical presence of a monopole-receiving antenna, used in measurements, is taking into account by the wire model while aperture arrays are described by the air-vent model.

The paper is organized as follows. In Section II, experimental procedure of measuring shielding effectiveness with tracking generator and spectrum analyzer is outlined. Section III and IV are engaged to the physical enclosure model and the numerical one. Section V provides discussion of the results. Finally, Section VI summarizes the work.

II. EXPERIMENTAL PROCEDURE

Usually, anechoic rooms are used to measure EM radiation of electronic equipment, as well as to test immunity. For instance, resistance of equipment to external radiation or resistance of equipment under test (EUT) irradiated by a controlled plane wave can be measured. Since interior space in anechoic room is coated with radio-frequency (RF) absorbent material, internal reflections are minimized and the device being tested is exposed to a precisely determined EM field. To measure the SE of enclosure, a spectrum analyzer or a scalar network analyzer can be used.

The measurements presented in this paper are performed in ordinary laboratory space by using RF absorbers. Also, unnecessary procedure of EM shielded chamber against external EMI is carried out. To determine the SE of enclosure a measuring procedure has to be performed twice, without and with enclosure. The SE is measured by the spectrum analyzer and with the S_{21n} and S_{21e} , parameters. The transmission parameters of the measurement without and with an enclosure are marked as S_{21n} and S_{21e} , respectively. The SE can be defined as in Eq. 1:

$$SE = 20 \log_{10} \frac{|S_{21n}|}{|S_{21e}|} \quad (1)$$

In order to find the best possible minimal interference in a measurement chamber, both transmitting antenna and enclosure are rotated. Since when the curve had sufficient low

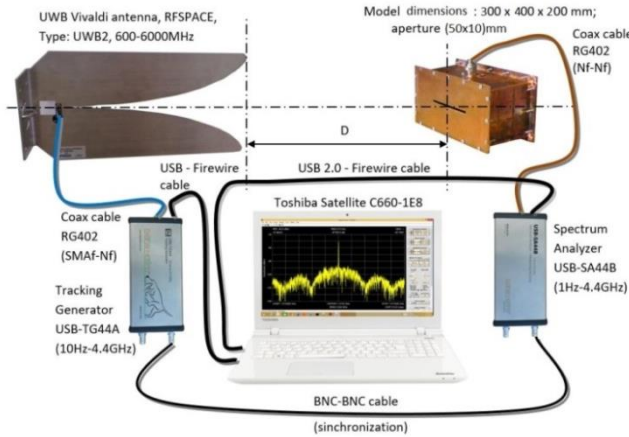


Fig. 1. The measuring configuration used in a semi-anechoic room.

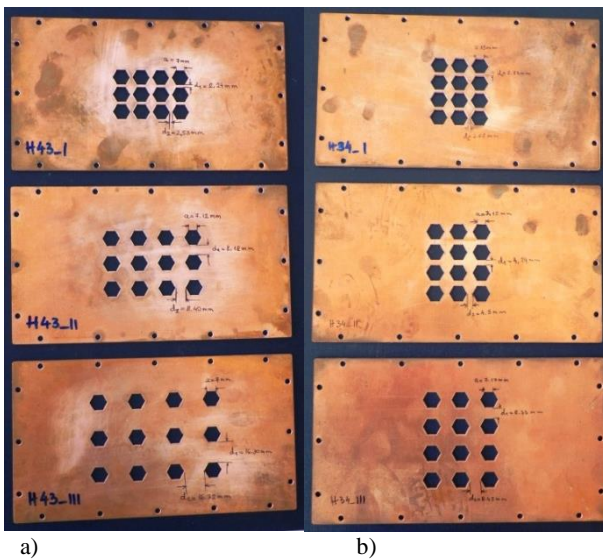


Fig. 2. Two sets of front panels with different air-vent distances;
a) H43 air-vent layouts, b) H34 air-vent layouts.

ripple of the s_{21} parameter, the measurement process is started. The enclosure is placed in far field against the transmitting antenna, in the whole observed frequency range [12].

The measurement processes are performed by using the spectrum analyzer with tracking generator and the SPIKE Software for PC computer, as shown in Fig. 1 [12]. A Vivaldi dipole antenna was used as a transmitting antenna, while an in-house monopole antenna was employed as a receiving one. The monopole, which is made of a copper material with a length of $l = 50$ mm and radius of $r = 0.1$ mm, is placed in the middle of the enclosure.

III. PHYSICAL MODEL

The rectangular metal enclosure with internal dimensions of (100 x 100 x 200) mm and with walls thickness of $t = 2$ mm is manufactured from copper material. This metal enclosure has removable front wall. Two sets of three panels are made. Each of the front walls is perforated with twelve hexagonal aperture arrays which are placed around the middle of a wall, Fig. 2.

In the first scenario, there are three panels of hexagonal air-vents formed in the group of 4×3 , as depicted in Fig. 2a. These front walls are used in experimental measurements. In order to make it easier to describe distances between any two hexagonal apertures, in both the vertical, d_1 , and the horizontal axes, d_2 , panels are labeled in the following order:

H43_I – width side of hexagon is $a = 7.0$ mm, aperture distances $d_1 = 2.24$ mm, $d_2 = 2.53$ mm and $cov = 0.5348$.

H43_II – width side of hexagon is $a = 7.12$ mm, aperture distances $d_1 = 8.18$ mm, $d_2 = 8.40$ mm, and $cov = 0.2833$.

H43_III – width side of hexagon is $a = 7.04$ mm, aperture distances $d_1 = 16.30$ mm, $d_2 = 16.32$ mm and $cov = 0.1487$.

For the second scenario, the same number of hexagonal air-vents is formed in the group of 3×4 . The panels are shown in Fig. 2b. In the following, more details about parameters of this group:

H34_I – width side of hexagon is $a = 7.12$ mm, aperture distances $d_1 = 2.33$ mm, $d_2 = 2.62$ mm and $cov = 0.5108$.

H34_II – width side of hexagon is $a = 7.15$ mm, aperture distances $d_1 = 4.24$ mm, $d_2 = 4.5$ mm and $cov = 0.4250$.

H34_III – width side of hexagon is $a = 7.17$ mm, aperture distances $d_1 = 8.33$ mm, $d_2 = 8.45$ mm and $cov = 0.2826$.

IV. NUMERICAL SIMULATION

In this paper, the TLM method is employed for numerical simulations. According to the physical enclosure model a numerical one is created. A compact air-vent model was used to model group of hexagonal shaped apertures. A TLM wire model was used to model a monopole-receiving antenna inside the enclosure.

The compact TLM air-vent model consists of two reactive circuits per propagation direction, which are placed between two neighboring TLM cells. The TLM cells coincide with the position of perforated metal wall. Firstly, it was developed for square and circular perforations on thin metal walls and on walls of significant thickness [10]. Afterwards, it was extended for rectangular and hexagonal air-vents [11].

The compact TLM wire model is employed for modeling an antenna inside enclosure. The main purpose of a receiving antenna is to measure the EM field level and its distribution. A receiving antenna is modeled as a wire segment which is incorporated into the Symmetrical Condensed Node (SCN) [8], [9]. The impedances of additional wire network link and short-circuit stub lines depend on the space used and time-step discretization, and also on per-unit length wire capacitance and inductance [11]. Two-way coupling between signal in the wire circuit and external EM field is described by pulses in transmission line network of SCN [10], [11].

In the considered model, the wire is connected to the ground via resistor R. The current which is induced on the wire, due to external EM field, generates voltage on the resistor R, which is loaded at wire base, and this allows measuring the level of EM field.

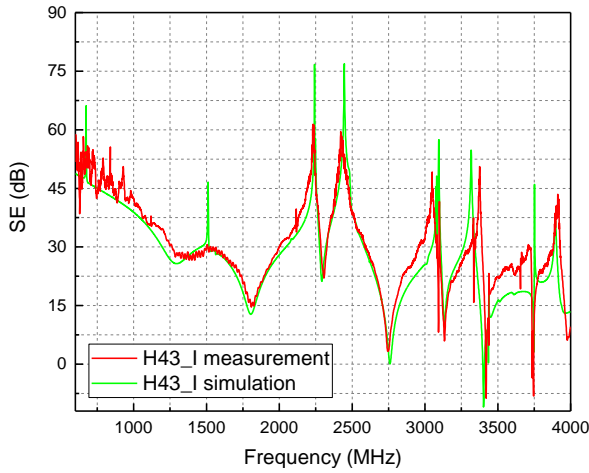


Fig. 3. Compared SE curves of **H43_I** enclosure model.

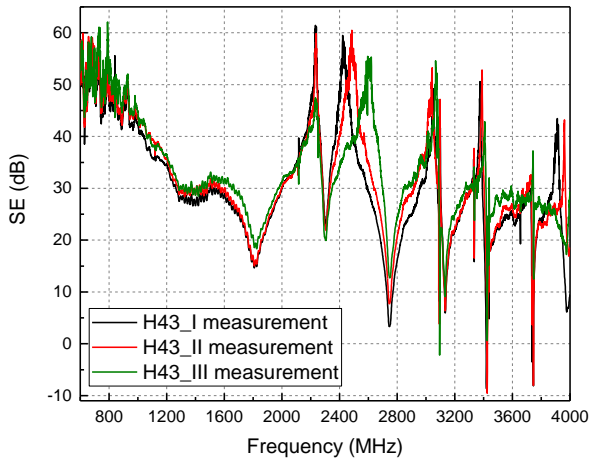


Fig. 4. Compared measurement SE curves for **H43** enclosure scenario against vertical incident plane wave.

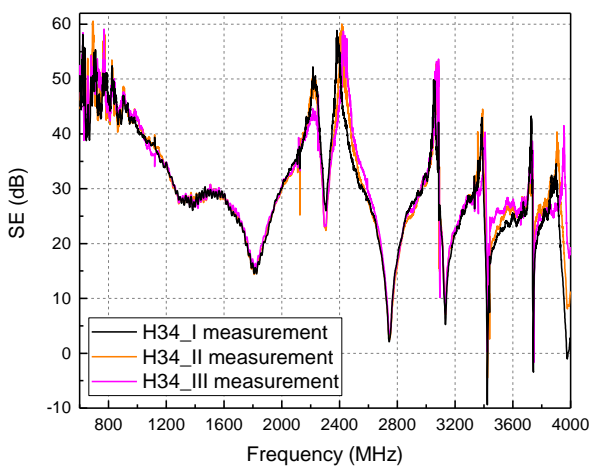


Fig. 5. Compared measurement SE curves for **H34** enclosure scenario against vertical incident plane wave.

The numerical TLM enclosure model is created according to dimensions, thickness, material and distance between air-vents like in physical one. The enclosure is excited by vertically polarized incident plane wave.

The SE characteristic is calculated as logarithmic ratio of the electric field without and with the enclosure, in the same probe point. A monopole-receiving antenna is placed in the middle of the enclosure to detect the electric field level. In the case of monopole antenna in free space, the size of a ground plane is chosen to be as the size of the enclosure wall when monopole antenna is placed inside the enclosure [10].

V. DISCUSSION OF RESULTS

In this section, we discuss about the experimental and the numerical SE results obtained for the considered enclosure. The analyses are carried out for two scenarios. In both, the front enclosure wall is perforated with 12 hexagonal air-vents. However, distances between the air-vents differ among panels. Both the numerical and the experimental analyses are conducted in order to improve the effectiveness of enclosure. The excitation toward the enclosure is normal incident plane wave vertically polarized. The frequency range of interest is from 600 MHz up to 4 GHz.

To start with, we consider the same enclosure model with three hexagonal air-vent layouts. It can be seen that the frontal panels differ between each other due to aperture distances, as illustrated in Fig. 2a. In the first scenario, the air-vents are arranged in groups of 4x3 around the center of frontal enclosure wall. Parameters of layouts entitled by **H43_I**, **H43_II** and **H43_III** are given in details in Section III. For instance, the first panel under the title **H43_I** has aperture distances mutually separated by the distance of $d_1 = 2.24$ mm and $d_2 = 2.545$ mm in vertical and horizontal directions, respectively. Therefore, the percentage of surface area covered by apertures is equal to 53.48 %. In numerical model, to describe the part of the perforated wall, the compact TLM air-vent model is employed. Figure 3 presents the SE results obtained by the measurement and the numerical simulation of the enclosure model **H43_I**. It can be observed an excellent agreement between compared shielding characteristics. Also, the experimental and the numerical SE curves which are obtained for other layout cases fit very well, so there is no need to display them.

Figure 4 illustrates the comparison of SE measurement curves for three different **H43** enclosure layouts. It can be noticed that all SE curves match very good at resonant frequencies. However, the SE levels are slightly higher with increasing in the distances between air-vents. Although, the resonances are almost the same, the SE peaks are shifted toward the higher frequencies, at frequencies around 2.4 GHz. This effect is occurred due to the reducing the coverage of perforated wall. Namely, the coverage in descending order is considered, from 53.48% up to 14.87 %.

The second scenario presents the air-vents in groups of 3x4 around the center of front wall of considered enclosure. The front panels are depicted in Fig. 2b. In this scenario, the distances between air-vents and the coverage of panels

This work has been partially supported by the Ministry for Education, Science and Technological Development of Serbia; project number TR32052, by the EUROWEB+ project and by the COST IC 1407 Action.

REFERENCES

- [1] C. Christopoulos, *Principles and Techniques of Electromagnetic Compatibility*, 2nd ed., CRS Press, 2007.
- [2] M. Li, J. Nuebel, J. L. Drewniak, R. E. DuBroff, T. H. Hubing, T. P. Van Doren, "EMI from Airflow Aperture Arrays in Shielding Enclosures—Experiments, FDTD, and MoM Modelling", *IEEE Trans. on EMC*, vol. 42, no. 3, pp. 265-2275, 2000.
- [3] M. Li, J. Nuebel, J. L. Drewniak, R. E. DuBroff, T. H. Hubing, T. P. Van Doren, "EMI from cavity modes of shielding enclosures – FDTD modeling and measurements", *IEEE Trans. EMC*, vol. 42, no. 1, pp. 29–38, 2000.
- [4] S. Ali, D. S. Weile, T. Clupper, "Effect of near field radiators on the radiation leakage through perforated shields", *IEEE Trans. on EMC*, vol. 47, no. 2, pp. 367–373, 2005.
- [5] B. L. Nie, P. A. Du, Y. T. Yu and Z. Shi, "Study of the shielding properties of enclosures with apertures at higher frequencies using the transmission-line modeling method", *IEEE Trans. on EMC*, vol. 53, no.1, pp. 73–81, 2011.
- [6] P. M. Robinson, M. T. Benson, C. Christopoulos, F. J. Dawson, D. M. Ganley, C. A. Marvin, J. S. Porter, P. W. Thomas, "Analytical formulation for the shielding effectiveness of enclosures with apertures", *IEEE Trans. on EMC*, vol. 40, no. 3, pp. 240–248, 1998.
- [7] J. Shim, D. G. Kam, J. H. Kwon, J. Kim, "Circuitual modeling and measurement of shielding effectiveness against oblique incident plane wave on apertures in multiple sides of rectangular enclosure", *IEEE Trans. EMC*, vol.52, no.3, pp. 566–577, 2010.
- [8] N.J.Nešić, N.S.Dončov, "Shielding Effectiveness Estimation by using Monopole-receiving Antenna and Comparison with Dipole Antenna", *DE GRUYTER Frequenz*, Vol. 70, Issue 5-6, pp. 191–201, April 2016.
- [9] N. Nešić, B. Milovanović, N. Dončov, V. Mandrić-Radivojević and S. Rupčić, "Improving Shielding Effectiveness of a Rectangular Metallic Enclosure with Aperture by Using Printed Dog-bone Dipole Structure," *52nd Int. Scien. Conf. Icest*, pp. 97-100, Serbia, Niš, June 28-30, 2017.
- [10] N. Doncov, A. J. Włodarczyk, R. Scaramuzza, V. Trenkic, "TLM modelling of perforated metal screens," *4th Int. Conf. Computational Electromagnetics*, Bournemouth, UK, 2002.
- [11] N. Doncov, B. Milovanovic, Z. Stankovic, "Extension of compact TLM air-vent model on rectangular and hexagonal apertures," *ACES Journal*, vol. 26. No.1, pp. 64-72, 2011.
- [12] V.Mandrić-Radivojević, S.Rupčić, N.Nešić, V. Alilović, "The shielding effectiveness measurements of a rectangular enclosure perforated with slot aperture", *Proc. of SST 2017*, pp.121-126, October 18-20, Osijek, Croatia.
- [13] N. J. Nešić / N. S. Dončov, "Analysis of TLM Air-vent Model Applicability to EMC Problems for Normal Incident Plane Wave", *Telfor Journal*, t. 8, br. 2, pp. 104-109, 2016.
- [14] N. J. Nešić "Numerical and experimental analysis of aperture arrays impact on the shielding effectiveness of metal enclosures in microwave frequency range", *Doctoral thesis*, in serbian, Singidunum University, Belgrade, 2017.

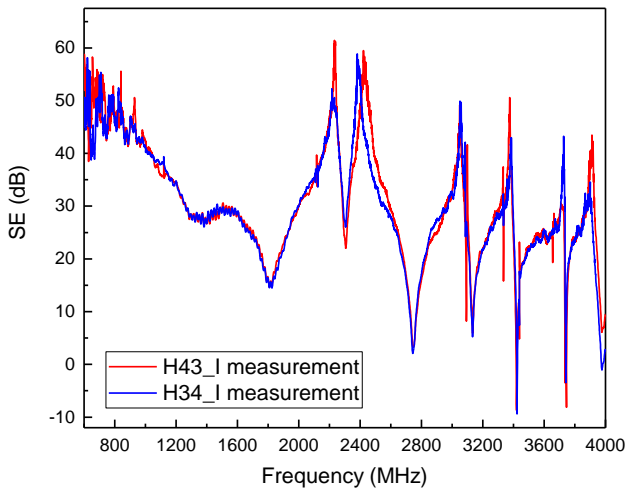


Fig. 6. Compared measurement SE curves for **H43_I** and **H34_I** enclosure models.

entitled **H34_I**, **H34_II** and **H34_III** are given in Section III. Like in the previous scenario, the measurement SE curves fit very well in comparison to the SE simulation results. Therefore, only experimental SE results are mutually compared for three cases, and they are presented in Fig. 5. It can be noticed that the SE characteristics are not significantly changed with increasing in distance between the air-vents. It can be explained that there are not a big difference in value between **H34_I** and **H34_II** coverages. However, due to decreasing in the coverage up to 0.2826 (**H34_III**), the levels of SE differ a bit at higher frequencies, especially at peaks. Beside this, the SE characteristics have the same values of the resonant frequencies for all three considered **H34** enclosure layouts. Detailed theoretical analysis of these issues is described in [13], [14].

Further, comparison between measurement SE curves of **H43_I** layout and **H34_I** layout are presented in Fig. 6. It shows excellent matching curves for almost the same spacing between the air-vents and similar coverage, even when the air-vent arrangement is turned; in one case it is 3x4 and the other one is 4x3.

VI. CONCLUSION

To conclude, the experimental results obtained for the considered enclosure are in an excellent match with the numerical ones. The TLM method incorporated with the TLM wire model and the TLM air-vent model is accurate and fast computer tool for efficient numerical characterization of EM problems on the field of EMC. It can be seen a remarkable matching between compared methods, especially at the resonance frequencies. Also, detailed analysis of the measured and numerical results shows very similar SE characteristics. It can be concluded that for a similar coverage value, even when the arrangement of the air-vents are reversed, the SE curves are quite similar.